

Stress form of Richard's equation for assessing plant's response to the abiotic stressors' relative extremes

Hegazy, El-Sh. M.

Ph. D. Natural Resources, Cairo University, Giza, Egypt

Abstract

The SSIMOD assumes that time and/or depth is a moisture. Accordingly, under deficit irrigation, the soil moisture regimes should be adopted without causing a reliable change in crop yield and plantations depend on four newborn abiotic stress parameters. The abiotic stress parameters are dependent variables of the geotemporal signals' interaction. A strong correlation between soil stress index and plant stress index was found. As plant stress index is the dependent variable of soil stress index, values of plant stress index were predicted using the corresponding values of soil stress index. Discretization equations between SSI and PSI were created in one and two dimensions. The stress form of Richard's equation in temporal variabilities was solved using the finite volume approximation. Relativity and hysteresis were found and discussed using the optimal approaches of modeling. The root water and nutrients' uptake, SSI, PSI, b_z , and b_t exhibited intrinsic variabilities. These hysteric effects may be attributed to the geosignal of total soil water energy. Silicon foliar application is a common managerial practice under such environmentally abiotic stressed conditions. Silicon enhances the plants' moisture status under combined drought and saline conditions.

Keywords: Global Climatic Changes, Drought, Salinity, Stress Form of Richard's Equations, Silicon

Abbreviations: RE: Richard's Equations, SF_RE: Stress Form of Richard's Equation

1. Introduction

Anthropogenic emissions of greenhouse gasses are pushing the Earth's climate toward a warmer state not seen for millions of years. The dependence on paleo climates allows to predict the future of our warming planet. These periods in Earth's past hold extremes of temperatures, precipitation patterns, cryospheric extent, and biosphere adaptations (Tierney *et al.*, 2020). In agro ecosystems, floods, drought, salinity, alkalinity, saline water intrusion, desertification, deforestation, heat shock, and storms are some examples not a survey. Accordingly, the world

will be facing the resurrection (Farnsworth *et al.*, 2023) or relativity forces will be interfering to halt the interrelated driving forces of transported phenomena letting the life on the planet Earth to continue seeking a new state of equilibrium (Fig. 1.1).

MENA countries face extremely climatic events now and then. Desertification and salinization in Egypt and Lybia, Daniel storms in Lybia, sea level rise and saline water intrusion in north Africa countries, alternative drought and storm in Somalia, soil salinization in Ethiopia, and desertification in Iraq, Syria, Turkey, and Lybia (Abaghandura *et al.*, 2017) are examples. Sandy dunes in arid lands (Fig. 1.2) are the main source of sandy and dusty storms.


***Corresponding author: El-Shazly M. Hegazy**

Email: shazlygouzouly@yahoo.com

Received: January 31, 2024; Accepted: March 27, 2024;

Published online: March 31, 2024.

©Published by South Valley University.

This is an open access article licensed under 

These storms increase soil salinity, water logging, and widespread rangeland degradation. They are hindering the physiological functions of plants during photosynthesis, pollination, and inflorescence. The percent of degraded land by desertification to the total surface area is 92% in Iraq, 10% in Syria, 100% in UAE. Saudi Arabia in particular is vulnerable to desertification. Because 76 % of the country's territories are nonarable lands, of which, 38 % is made up by deserts (Haktanır et al., 2004). In Egypt, desertification is a common climatic change problem. Where the Nile valley becomes narrower, the Aeolian depositions of sand will extend. The alluvial Nile clay will be being buried under sandy textured deposits. Therefore, the soil profile will be characterized with two diagnostic horizons. A: Aeolian Fine Sandy Deposits. B: Alluvial Clayey Nile Deposits. Spatial variabilities in water uptake, nutrients' uptake, and HASP (Hegazy, 2024) won't be being induced due to the prevalence of the fast drainable porosity of non-hysteric sandy A horizon whereas being induced by the prevalence of the fine storage porosity in alluvial hysteric clayey B horizon. This is because: 1) On each depth and time is a unique value of each moisture and achieved HASP. 2) Processes sorption is time, depth and temperature dependent. 3) Absent of hydrodynamic dispersion in A horizon and the opposite is true for B horizon. In El-Kobanyia village, Aswan governorate, Egypt, HASP, may be governed by three types of water flow through heterogeneous porous media each of which has its characterized concepts and governed equations. Accordingly, water flow in this case is a piecewise function of depth. They are as follow:

- Water flow through non hysteric sandy A horizon (Bazaraa, 2015).
- Water flow through hysteric clayey B horizon (Bazaraa, 2015).
- Water flow through sand- water and water- clay interfaces (El-Khader, 2015)

Silicon, the seventh most abundant element in the universe, plays vital rolls in saving planet Earth against the negative impacts of the global climatic changes as follows:

- Many marine creatures require silica to produce their skeletons. For instance, phytoplankton float near the ocean's surface and capture carbon dioxide through photosynthesis. Without a steady supply of silicon from rivers, deep-sea vents, and other sources, these organisms would not be able to produce the biogenic opal that forms their skeletons. When diatoms and other plankton die, they sink to the bottom of the ocean, and their skeletons are buried in marine sediment (Biard *et al.*, 2018). The phytoplankton are very sensitive to climatic changes especially temperature rises,
- Treating the sulfuric acid aerosols in the stratosphere with silica aerosols reduces significantly the short incoming radiation. Accordingly, increases the Mie scattering of the stratosphere.
- Silicon on plant leaves could act as antenna reflects the solar short incoming radiation. Accordingly, reducing the impact of global temperature rise by cooling plant leaves,
- Treating soil with silica enhances soil physical and hydro-physical properties (Hegazy 2002), plant growth, and root water and nutrients' uptake under optimal and extreme conditions (Epstien, 2009 and El-Sokkary, 2018). In the case of cultivating silicon accumulator crops such as sugar cane, great amounts of silicon are removed from soils and they should be returned back by recycling agricultural wastes. Otherwise, impacts of global temperature rise on the pedoclimate may be extended.
- Silicon could help in protecting humans, animals, and plants from the biotic attack and diseases.
- In El-Kobanyia, Aswan, Egypt, the alluvial Nile clay is buried under the aeolian Sahara sand through the process desertification.

The latter is a common climatic change problem in the arid and semi-arid zones. In my opinion, continuous planting of sugarcane crop for five years is the best way of reclamation the soil desertification there. . Incorporating sand with synthetic conditioners will improve the soil physical and hydrophysical properties on one hand. On the other hand, sugarcane, the silicon accumulator crop, will build its biomass from underground alluvial Nile clay. After harvesting the crop, its residual ash and mud should be returned institute. On the other words, the sugarcane has used the improved soil hydraulic capacitance, by adding synthetic conditioners, to lift the skeletal clay raw material from subsurface bringing it to the surface as mud and ash. Simply, sugarcane is being acted as a clay's phytoupump used for treating the problem of soil desertification without the interaction of agricultural machinery.

Under the stressed conditions of climatic changes, converting the well known Richard's equation to a new stress form one by replacing the absolute values of total soil water energy with total relative extreme ones is a type of biophysical simulation. The simulation using the relative extreme values is taking into consideration the values of total soil water energy under stressed conditions relative to their values under optimum conditions. The optimum condition of total soil water energy represents the ideal wetness for achieving potential yield and transpiration. It depends on soil type, plant type, plant species, plant age, and atmospheric forces. Soil moisture changes across the unsaturated zone because of: 1) Inflow of source or gaining water via infiltration from the surface due to rainfall and irrigation. 2) The outflow of sink water caused by evapotranspiration and percolation beneath the root zone. Richards'

equation represents the most commonly used model for soil moisture dynamics in the unsaturated zone. As it is used to quantify fluxes in the vadose zone, an accurate characterization of the soil water dynamics is required. Recently, stress form of Richard's equation (SF_RE) was developed in order to distinguish the water flow characteristics in variably saturated zone using Hegazy abiotic stressors' parameters (HASP) (Hegazy, 2024). Variabilities in HASP represent the responses of agroecosystem components, plant and soil, toward the naturally or artificially applied total relative extremes.

The variably saturated flow is the link between surface water and groundwater. Groundwater in the non-artesian aquifers is divided into saturated and vadose zones. Most of the groundwater in the saturated zone is replenished from seepage from the variably saturated zone. Hence, the study of groundwater resources will have to account for the flow in both zones in interaction with each other. The movement of groundwater in the saturated zone is described by Laplace's equation, while the movement in the variably saturated zone is described by Richard's equation. Both analytical and numerical solution of RE are complex because of the strong nonlinear relationships that link between soil moisture and soil hydraulic conductivity on one side and soil matric-potential on the other side (Berardi *et al.*, 2022). Another difficulty is that as we approach the saturation surface of non-artesian aquifers, the Richards equation degenerates into a Laplace equation with completely different mathematical properties.

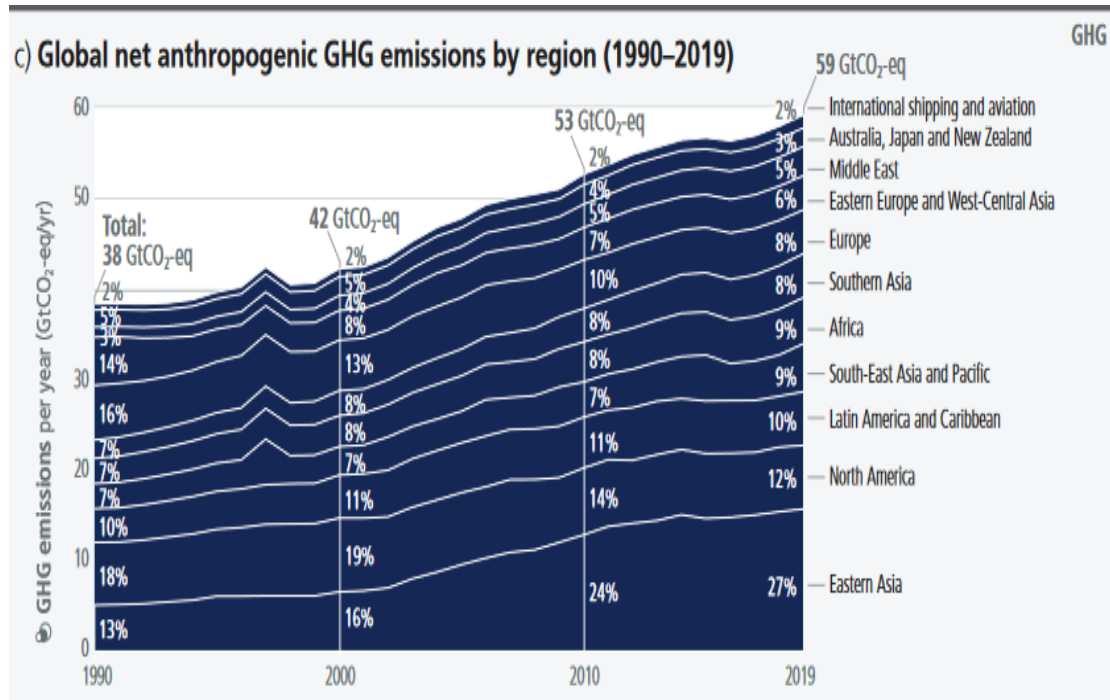


Figure (1.1): Global net anthropogenic GHG emissions by regions (1990- 2019) (IPCC, 2023).

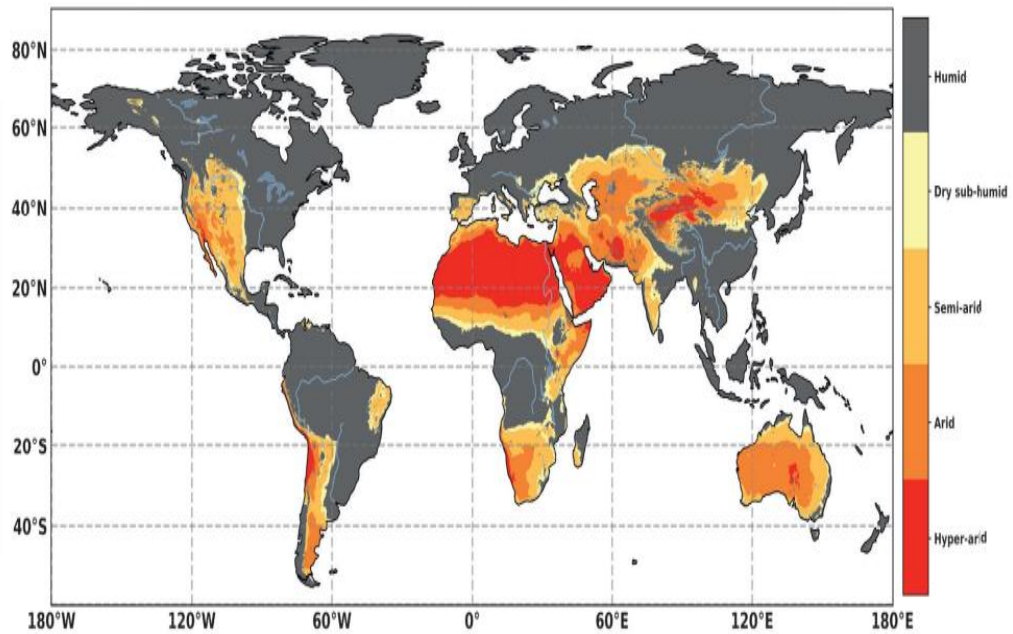


Figure (1.2): Geographical distribution of drylands, delimited based on the aridity index (IPCC, 2023).

Than and Song (2023) introduced an algorithm for solving the one-dimensional Richards equation using the finite volume method. By using that algorithm, the unsaturated and saturated zones interact to determine the exact position of the water table. Analytical solutions of RE are valid for simple conditions. This is because of the high nonlinearity of RE which make the analytical solution not possible but for special cases. Instead, numerical methods are used in order to solve the unsaturated flow equation in the last thirty years. Finite difference and finite Element solutions were faced to some degree of mass balance errors, numerical oscillations, and dispersion. While finite difference method is useful in one dimensional numerical solution because it doesn't need mass lumping to minimize oscillations, finite element is preferred in two- and three-dimensional flow domains (Pour *et al.*, 2011).

The subjects of that research chapter are as follow:

- A. Study the nonlinear normal distribution of soil stress index with time or depth as a moisture.
- B. Macroscopic study of the effect of soil salinization on the nonlinear distribution of soil water redistribution under silicon managerial practices.
- C. Solve the stress form of Richard's equation.
- D. Develop discretized equations SSI& PSI in one and two dimensions.
- E. Develop a statistical model of SSI& PSI using the regression analysis.
- F. Study the intrinsic variability from the optimal approach of modeling.

2. Materials and Methods

Predicting the effects of climatic changes on the agro-ecosystem continuum could be done by taking the data from the past, the most dried year

(2009/ 2010). An open field experiment was done in the most dried year 2009/2010 in Oraby Village, Maryout area, Alexandria, Egypt. The negative impacts of drought and salinity on wheat plants (*Triticum aestivum* L.) cultivar, were managed by applying silicate fertilizers. The foliar application of silicate fertilizers is recommended due to abiotic stressed conditions (Hegazy, 2023). Potassium silicate and sodium silicate fertilizers were sprayed in three concentrations 0.0, 30.6, and 40.8 ppm as silicon. All of them were foliarly sprayed at ages 45, 60, and 75 days from seed emergence at the early morning. The 6 treatment combinations were distributed in 3 salinity levels, 3.12, 4.82, and 5.12 dS/m, in a split-split plot design with four replicates. The ET_C was calculated from metrological data according to FAO (2002). The irrigation intervals were each 20: 25 day. Wheat plants faced a naturally applied drought by the end of each irrigation cycle. SF-RE was created by the author contains four abiotic stress parameters, SSI, β , bz, and bt (Hegazy, 2024). SSI and bz were estimated. A statistical model between SSI and PSI was created using Excel 2007. Estimating the indices of plant and soil and the relation between them were done according to Hegazy (2020). Seasonal root distribution, Sbz (cm/MPa, cm/cmH₂O...etc.), could simply be obtained by dividing $0.75dz/h^*$ (Hegazy, 2024). SF-RE was solved in two dimensions (t, z) using the assumptions of finite control volume (Pour *et al.*, 2011). The discretization equations between the indices of plant and soil were achieved by the author. Hysteresis and Albert Einstein's relativity (intrinsic relativity) were discussed using the optimal approach of modeling (Dubbart *et al.*, 2023).

3. Results and discussion

3.1. Water Redistributions in SSIMOD Follows the S Shaped Water Stress Response Function of Van-Genuchten.

Figure (3.1a) illustrates that the SSI followed the general trend of S shaped plant response function of Van-Genuchten (1987); this may be attributed to:

- SSI which accounts for the relative total soil potential under stressed and unstressed conditions, respectively, and determines the quantities and the mechanisms of water and nutrients removed from the soil for building yield.
- The plant response function which accounts for the relative yields under soil stress and unstressed conditions, respectively.
- Both indices are fractionally dimensionless and oscillates from zero to one, theoretically.
- The hysteresis phenomenon in soil stress index (Figs. 3.4 and 3.5) which is the resultant of the known hysteresis in the water retention curve during wetting and drying cycles.
- The difference in total soil potential needed for reaching maximum plant growth as the soil dries day by day during drainage is less than the difference in total soil potential needed for reaching maximum plant growth as soil waters during irrigation (Fig. 3.1a). This means a hysteresis phenomenon in plant stress response function during wetting and drying cycles. Accordingly, root water uptake ($S=\beta.SSI$), and leaves transpiration exhibited hysteric relationships (Zarebanadkouki *et al.*, 2018; Wang *et al.*, 2020). These hysteric effects may be attributed to the inherent hysteresis in soil water retention, SSI, and therefore PSI.
- It's the moisture redistribution (bz) which makes the curvature of SSI becomes gradual

and hence saves plants life as long as possible now and then each wetting drying cycle. It's the gaining factor (bt) which determines the moisture regimes should be applied in the deficit irrigation scenarios without causing a reliable reduction in crop yield and plantation properties(Fig.3.1f). Finally, it's the soil stress index or soil water hydraulic capacitance which determine the type and amount of water and nutrients' uptake in accordance with stress or stress, strain, and weathered controlled forces, respectively.

But there are some limitations between the water stress response function of Van- Genuchten and soil stress index model, this limitation is as follows: As the change in SSI is sharp whereas the change in water stress response function is gradual, root deeply extends for categorizing the energy states of soil water to water. That sharpness is due to the surface layer which loses its moisture content from saturated to satiated conditions in 2:3 days (Fig. 3.1a). From the second day to the third one, SSI reaches its relative maxima and then sharply declines due to evapotranspiration. As SSI reaches its relative minima at the end of the third day, water stress appears and accordingly plant root starts to do on a response function by deeply extending the soil profile (creating the variably saturated zone) categorizing soil moisture to water and nourish. Each new incoming soil layer, plant roots do what they have done in the outgoing ones now and again.

On the other hand, soil layers are not separated which means a process of moisture redistribution does occur now and then creating the three zones of abiotic stress (Hegazy, 2020).

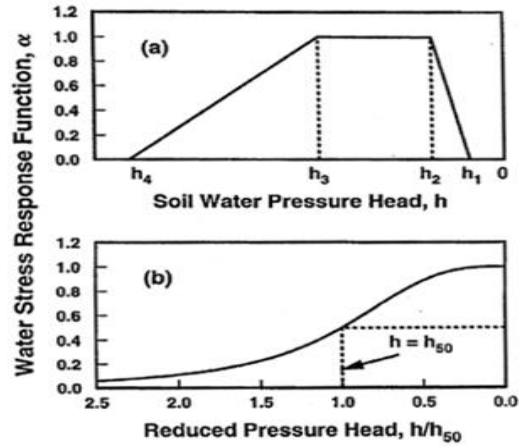
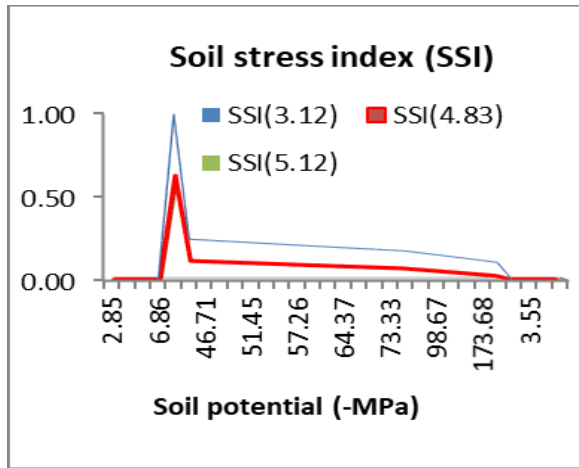


Figure (3.1a). The variation of SSI without moisture redistribution(left) and water stress response function (right) due to Feddes *et al.* (1978) (a) and Van-Genuchten, (1987) (b) All with total soil Potential variation.

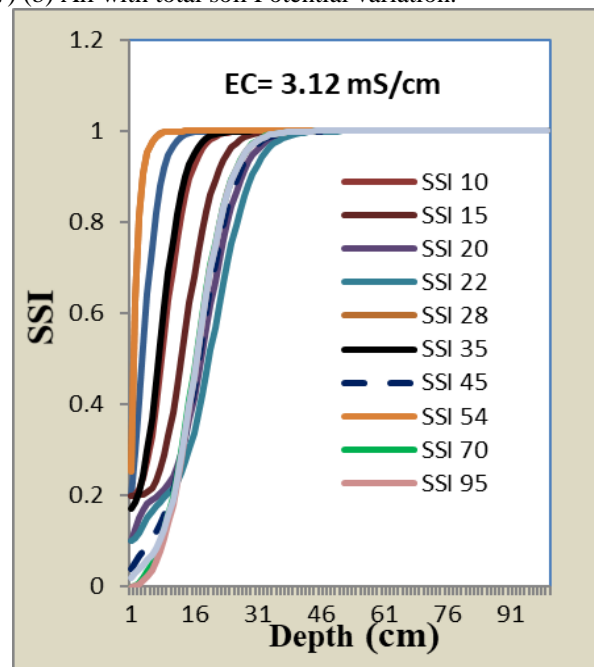
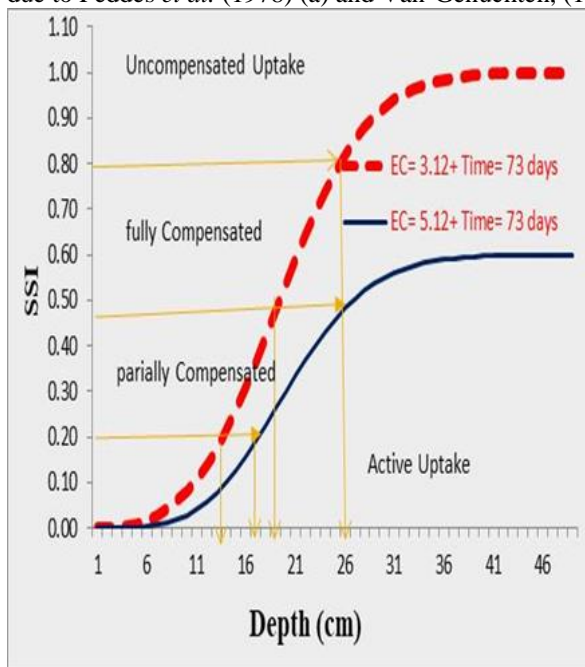


Figure (3.1b): The SSI variation with depth at the same time. The S shaped development of SSI with depth. SSI’s logical model of water and geo-alkaloids’ uptake.

Figure (3.1c): The SSI variations with time, depth, and moisture redistribution in non-saline soil. They follow the S-shaped of Van-Genuchten.

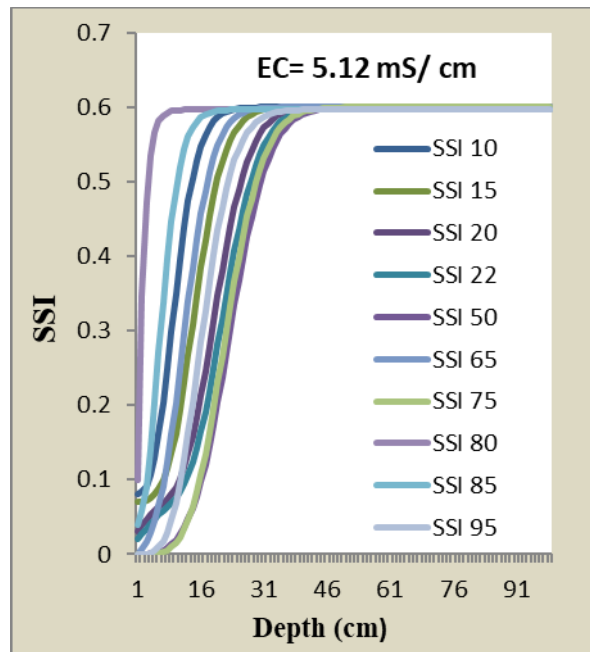


Figure (3.1d): The SSI variations with time, depth, and moisture redistribution in saline soil. They follow the S-shaped of Van- Genuchten.

In logical modeling of the response of root uptake under stressed conditions, it has been primarily imposed that the uptake becomes zero at water logging conditions of the capillary fringe zone, water table zone, and a part of the variably saturated zone which holds moisture content exceeds the equivalent moisture of field capacity. Also, it has been imposed that the non-compensated root uptake occurs at SSI 0.8: less than 1.0, fully compensated root uptake at SSI 0.5: 0.8, partially compensated root uptake at SSI 0.2: 0.5, and active uptake at SSI < 0.2 (Fig. 3.1b). The value of SSI differs from cycle to another at the same time and depth. This may be attributed to the change of crop coefficient from one month to another, hysteresis, and relativity phenomena in soil potential and SSI (Figs. 3.1c and 3.1d).

As depth is a potential which means that at surface soil system becomes in a highly negative total potential due to evapotranspiration and redistribution and this potential becomes less negative as the depth increases until reaching the constantly shaped soil moisture profile which means a steady state condition of soil water redistribution tensor. The term $b(z)$ may give

details about water redistribution and accordingly root distribution (Fig. 3.1f). In Egypt, desertification is a common climatic changes problem. Where the Nile valley becomes narrower, the Aeolian depositions of sand will extend. The alluvial Nile clay will be being buried under fine textured sandy deposits. Therefore, the soil profile will characterized with two diagnostic horizons. A: Aeolian Fine Sandy Deposits. B: Alluvial Clayey Nile Deposits. Spatial variabilities in HASP will be being induced due to the privilege of fast drainable pores in sandy A horizon whereas the previalge in alluvial clayey B horizon was for fine water stored pores. in El-Kobanyia village, Aswan governorate, Egypt, HASP, may be governed by three types of water flow through heterogeneous porous media each of which has its characterized concepts and governed equations. Accordingly, water flow in this case is a piecewise function of depth (Figs. 3.1b). They are as follow:

- 1) Water flow through non hysteric sandy A horizon (Bazaraa, 2015)
- 2) Water flow through hysteric clayey B horizon (Bazaraa, 2015)

3) Water flow through sand- water and water- clay interfaces (Fig. 3.1e) (El-

Khader, 2015).

$$\Delta p = p_a - p_w = \sigma_{aw} \left(\frac{1}{r_{c1}} + \frac{1}{r_{c2}} \right)$$

$$\sigma_{aw} \cdot \cos \psi = \sigma_{sa} - \sigma_{sw} ,$$

$$\Delta p = p_c = p_a - p_w = 2 \sigma_{aw} \cdot \cos \psi / r_c,$$

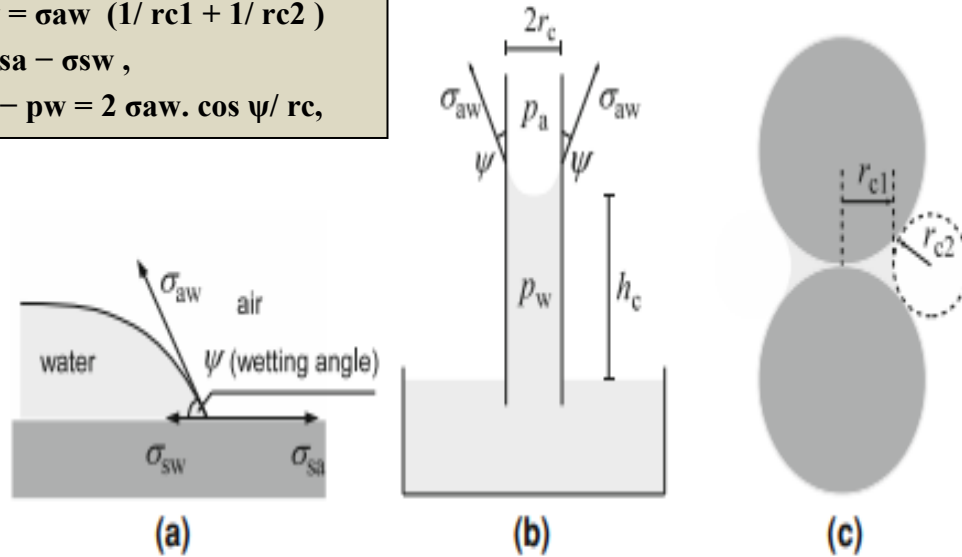


Figure (3.1e): The effects of free energy: A) Equilibrium position of the fluid–fluid interface near the solid surface, B) Rise of the wetting fluid in a capillary tube. (Source: Szymkiewicz, 2013).

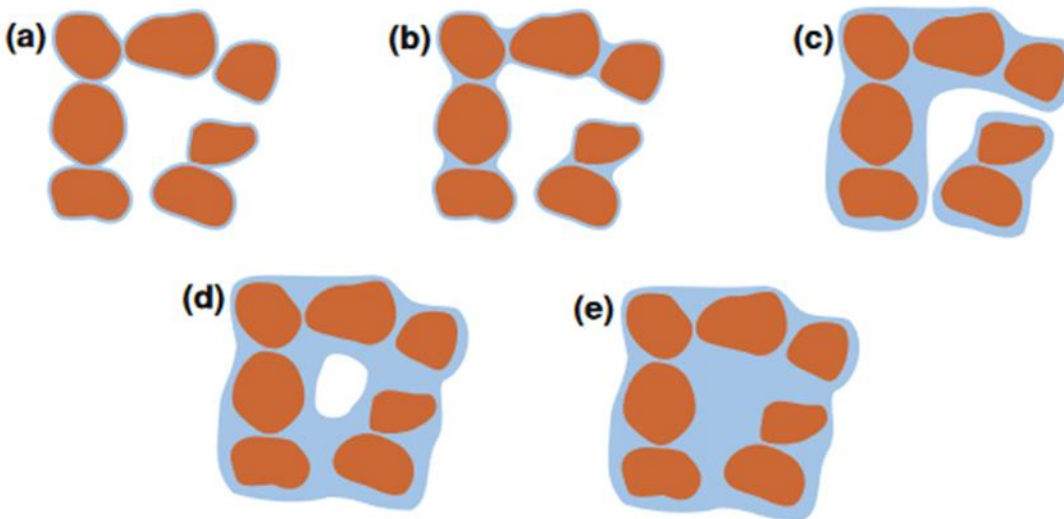


Figure (3.1f): Types of soil moisture regimes in variably saturated porous media: (a) adsorbed regime, (b) capillary pendular regime, (c) capillary funicular regime, (d) occluded air bubble regime, (e) fully saturated regime the start of saturation zone. (Source: Szymkiewicz, 2013).

3.1.1. Roots' Distributions Follow the Moisture Redistribution (bz)

In fact, salinity of soil solution increases its density, viscosity, pore water velocity, diffusivity, and hydraulic conductivity. This is

due to enhancing the vertical downward water flow by more dense liquid. Another fact, the attractions between water and solvent molecules may reduce the evapotranspirative losses. As the saline water reduces the actual evapotranspiration, it reduces root growth and

expansion too. Hence, salinity makes plants' roots unable to extend deeply to do their response of partially or fully water and nutrient compensation. In the optimality approach, root distribution should follow the water redistribution (Fig. 3.1f). Silicon improves the root distribution by allowing roots to navigate the soil system in a smooth way which enables roots to click the easiest path, the moist wider planar voids which are already dilated due to salinity, in searching and categorizing moisture to water and nourish (Peter 2016) and this is the reason that silicon enhancing the optimality saving the plant energy under stress conditions (Hegazy, 2022a, b). Accordingly, silicon, the earthy skeletal element, enhances the geobiosignals' interaction.

Figure (3.2) showed that soil salinity reduces seasonal root distribution. This is because the ability of roots to uptake water and nutrients under combined abiotic stressed conditions is functions of crop type, age, degree of tolerance and species, how much are regimes in the stressed parts (Fig. 3.1f), and how deep are they. Increasing the abiotic stress in a part of root domain reduces the uptake from it. As the root system is cooperative, the crop water and nutrients' demand is fully or partially compensated from unstressed or less stressed parts, respectively. As PSI is reduced in comparable with the SSI, the compensation of wheat's cooperative root system is partially (Fig. 3.3). Figure (3.2) also showed the role of potassium silicate fertilizers in increasing root distribution and water redistribution under moisture deficit conditions. While plant available water was depleting, plant roots elongated started to absorb water from less stressed parts of root zones (Albasha, 2015). Si depositions in the roots can increase cell wall elasticity during root cell elongation (Laing et al., 2007). Therefore, The geo-bio signals' interactions under abiotic stressed conditions are as follows:

- **The first type of soil response towards the applied stressor:** The interaction between ecosystem components, plant and soil; due to drought cycles, soil is shrinking its energy of field capacity now to the half of its value at the wetting cycles to save plant's life and prevent the hydrological release (Homaei et al., 2002, Radcliffe and Simunek, 2014, and Wang et al., 2020). when the total soil water energy decreases, soil stress index increases.
- **The second type of soil response towards the applied stressor;** ought to salinity, which affects negatively plantation properties and therefore yield components. Similarly, soil is shrinking its energy of field capacity again. These shrinkages extend deeply to the depth of 25 cm and continue to overwhelm the areas of zero root uptake and most active root uptake to save plant's life and prevent the hydrological release (Wang et al., 2020). The matched fact that rhizospheres are wetter than bulk soils during drying cycle, but remain temporarily dry after re-watering. This fact revealed that the hydraulic properties of the rhizosphere are time and depth-dependent (time is a moisture, water potential, root uptake, and therefore plant and soil stress indices) (Zarebanadkouki et al., 2018 and Wang et al., 2020). The latter hysteric effect matched the findings of Wu et al. (2020) who found that the actual transpiration (T_a) and relative transpiration ($PSI = T_a / T_p$) of stressed plants usually do not reach their maximum levels contemporarily with the instantly maintained soil water status after rewetting.
- **The third type of soil response towards the applied stressor;** drought concentrates the soil solution, increases its conductivity which is already high due to salinity stress, decreases the thickness of electric double layer, increases the diffused ions swarm discussed by Sposito (2008). The diffused

ion swarm satisfies the remaining charges of the soil particles electrostatically therefore, reduces the surface potential of highly energetic clayey particles. Hence, it reduces the free energy of the background soil solution. In fact, it reduces the free energy responsible for capillarity phenomenon. The latter three soil responses toward the applied abiotic stressors enhance plants to withstand against the abiotic stress conditions and complete their life cycle. The energy of field capacity is shrunk according to the optimal approaches of modeling (Dubbert et al., 2023).

▪ **The fourth type of soil response towards the applied stressors:**

The agro ecosystem creates a relativity in its properties to prevent the plants' hydrological release and plasmolysis.

3.2. SF-RE and Plant Stress Reduction Function

As soon as the data of daily SSI and PSI were estimated, an empirical regression response functions between them would be developed (Fig.3.3 and table 1). The SF-RE are as follows:

$$C (SSI) \frac{dSSI}{dt} = \left[\frac{b(t)}{b(z)} (dSSI + b(z)) \right] \frac{d}{dz} - \beta \cdot SSI \tag{1}$$

$$C (SSI) \frac{dSSI}{dt} = [k(h) (dSSI + b(z))]d / dz^2 - \beta \cdot SSI \tag{2}$$

$$C (SSI) \frac{dSSI}{dt} = [k(h) \frac{(dSSI+b(z))}{dz} \frac{d}{dz}] - \beta \cdot SSI \tag{3}$$

Where: S= $\beta \cdot SSI$ root water uptake, t, z: time and depth respectively, SSI: soil stress index, β : soil water hydraulic capacitance. c: soil water holding capacity (L^{-1}), Kh: unsaturated hydraulic conductivity ,

The macroscopic solution could be obtained by direct substitution in Rechar'd's equation as follows:

1. $SSI = \frac{(1+(\alpha\Psi)^n)^m}{(1+(\alpha\psi^*)^n)^m}$ (m=1/n)
2. Prediction of PSI values by the corresponding values of SSI (see section 3.3.2.1)
3. The water holding capacity, $c_{(SSI)}$, is the slop of PF-curve
4. The water redistribution $b(z) = (dz/h^*) = (L-L)/L^3=L^{-2}$. As soil water potential is expressed as water head.
5. The gaining factor $b(t) = k_{(h)}/h^* = (L/T)/L = T^{-1}$ the same unit of the source term
6. The unsaturated hydraulic conductivity, $Kh = \frac{b(t)}{b(z)} dz$
7. The potential transpiration T_p is calculated from the metrological data according to FAO (2002).

8. The soil water hydraulic capacitance $\beta = T_p / \mu = T_p \cdot (dSSI/ dPSI)$ is the only unknown. The slope of the grave in figure (3.2) is μ .
9. The sink term $S = \beta \cdot SSI$
10. The slope of the relation between SSI and PSI in the equations mentioned in Table (1) could be obtained by calculating the first order derivatives of these equations and could be considered as the synonyms of the proportional coefficient (μ) of the relationship between PSI and SSI.
11. When μ is being a variable, intrinsic variabilities will be appear. The values of SSI, PSI, β , water uptake, and nutrient uptake will differ while moving from wet to dry than from dry to wet. Another type of intrinsic variability may be appear, the Albert relativity.

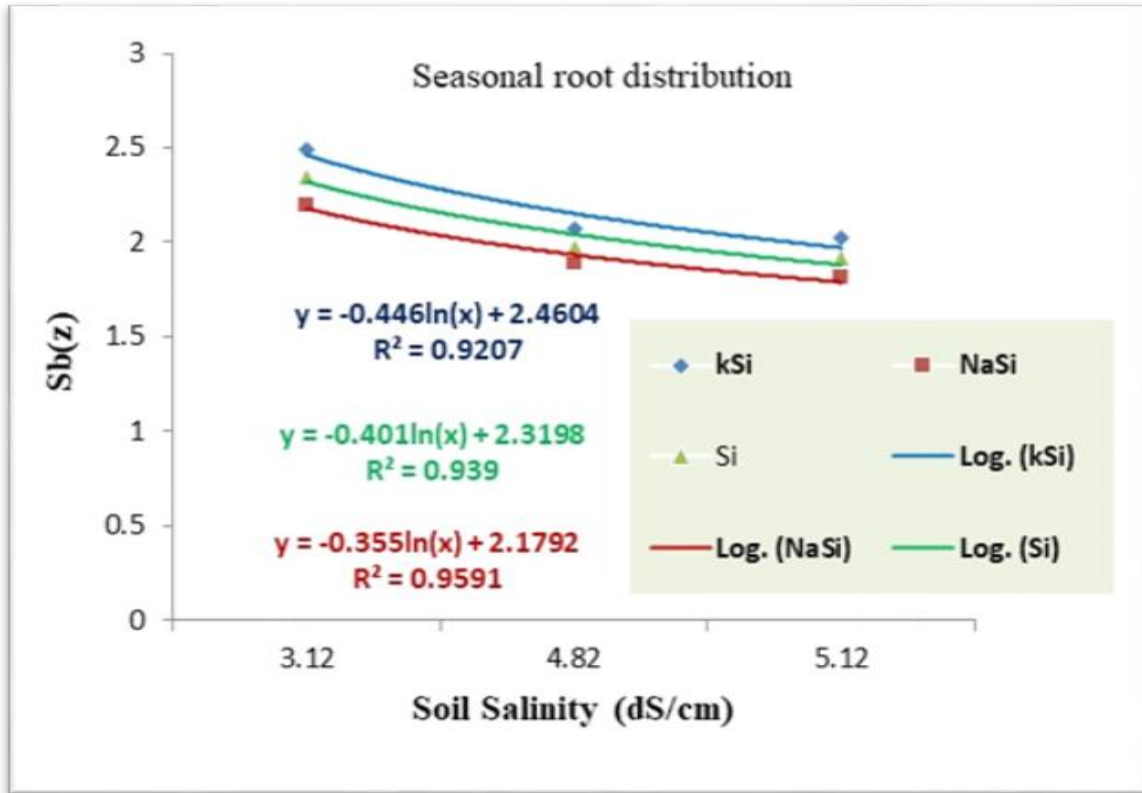


Figure (3.2): Seasonal root distribution as a response to silicon application under abiotic stress conditions. μ at the end of compensation

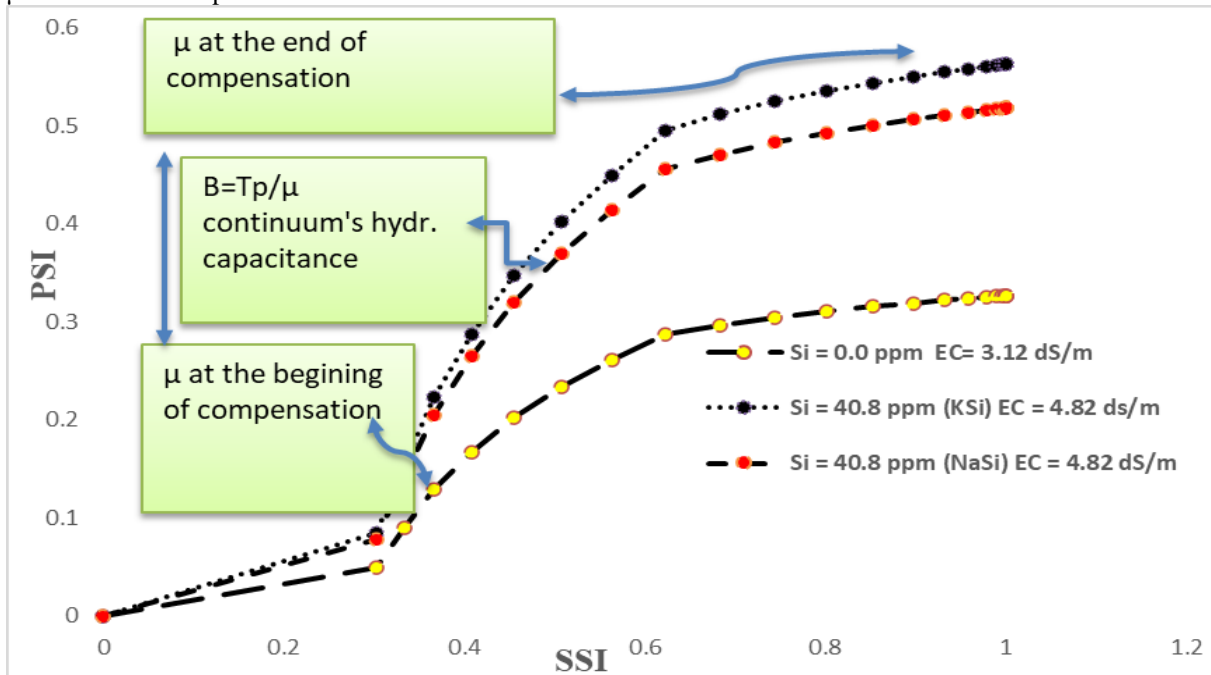


Figure (3.3): The variation of PSI with SSI at the first irrigation interval for fields of saline soil treated with silicon and non-saline soil with control silicon treatment.

Table 1. Estimation of μ , the proportional coefficient between PSI and SSI.

KSi	PSI=f (SSI)	$\mu= dPSI/dSSI$	R²
Logarithmic	$y = 0.2044\ln(x) - 0.0169$	$0.2/x$	0.95
Polynomial	$y = -0.4607x^2 + 1.1165x - 0.0819$	$0.92x+1.1165$	0.9329
Linear	$y = 0.555x + 0.0462$	0.555	0.8846
NaSi	PSI=f (SSI)	$\mu= dPSI/dSSI$	R²
Logarithmic	$y = 0.1881\ln(x) - 0.0156$	$0.188/x$	0.945
Polynomial	$y = -0.4239x^2 + 1.0272x - 0.075$	$-0.8478x+1.0272$	0.9329
linear	$y = 0.5106x + 0.0425$	0.5106	0.8846
Control	PSI=f (SSI)	$\mu= dPSI/dSSI$	R²
Logarithmic	$y = 0.1186\ln(x) - 0.0098$	$0.1189/x$	0.936
Polynomial	$y = -0.2672x^2 + 0.6476x - 0.0475$	$-0.5344x+0.6476$	0.9329
linear	$y = 0.3219x + 0.0268$	0.3219	0.8846

The values of daily SSI were high particularly in the subsoil and reached the value of one as a max. (Figs.3.1c, 3.1d, and 3.3), whereas the values of parallel daily and average PSI in all treatments were low and reached 0.6 as a max (Fig 3.3). This may be ascribed to the factors affecting the consumed energy by plants to combat stressors. SSI started to be high at a soil depth of 40 cm and, after that, matched the constantly shaped soil moisture profile's trend due to moisture redistribution (bz). This means that the variably saturated zone contains a dead short roots' area in which the roots' dependant cooperative pipes could not uptake water because of the harsh extreme stress conditions.

That decrease in water uptake may be compensated by the constantly shaped zone by long alive plants' roots which have dependent roots' suction too. This compensation is a response function to how much the fully stressed or partially stressed layers of the topsoil and variably saturated zone were, respectively. In addition, how deep the unstressed layers of the constantly shaped zone were. The latter compensation depends on many factors such as soil texture, structure, hydraulic conductivity, energy of soil water, evaporative demand, properties of plant roots such as rooting depth and radius (Peters, 2017), above ground plant properties (Jarvis, 2010), and other abiotic and biotic stresses than drought and salinity. These factors may control the consumed energy during categorizing the energy states of soil water by

plants' roots to compensate (Homaee *et al.*, 2002). Therefore, they hold the responsibility of low average and daily PSI values. In the case of heavy textured soil, harsh extreme topsoil, and deep variably saturated zone grown with crops which have short rooting depth and limited root elongation, the compensation may not overwhelm the decrease in potential uptake from the dead short roots' layers and therefore average and daily PSI may be reduced. In soil-plant- atmosphere continuum, free from any type of abiotic and biotic stressors but drought and salinity, the reduced PSI against the maximized SSI means a partial compensation did occur and the values of PSI were less than their critical value (Simunek and Hopmans, 2009).

The present study showed that SSI was better than PSI in describing the decrease in yield due to drought and salinity in a field free from other abiotic and biotic stressors. The interaction between drought, salinity, and oxygen deficit in soil system and other abiotic and biotic stresses (ultraviolet radiation, sunburn, temperature rises, storms, pathogens, and diseases) makes PSI better than SSI in describing the decrease in yield. This is because the plant is the final receiver of all stressors in the agroecosystem. This match the finding of Albasha *et al.* (2015) who concluded that compensated root uptake is independent of plant stress status and should be interpreted as a response to soil water status variability.

Hegazy abiotic stressors' parameters (HASP) will be helping for decades in managing vadose zone under irrigation deficit scenarios. For instance, the gained factor parameter (bt) will help the decision makers to figure out the soil moisture regimes should be adopted without causing significant reductions in crop yield and planation propertied(Fig. 3.1f). Soil water hydraulic capacitance will take the advance in ranking HASP. . This is because the incoming reasons:

- SWHC depends on soil stress index
- SWHC depends on plant stress index
- SWHC depends on potential transpiration
- SWHC depends on abiotic and biotic stressors in the root domain including the total energy states of soil water
- SWHC is suitable for assessing the impact of combined drought and salinity in agricultural fields full of biotic and abiotic stressors
- SWHC marks the type and amount of water and nutrients' uptake under combined biotic and abiotic stressors in accordance with stress, strain and weather controlled forces
- SSI depends only on the total energy states of soil water
- SSI is suitable for assessing the impact of combined drought and salinity in agricultural fields free of other biotic and abiotic stressors
- SSI marks the type and amount of water and nutrients' uptake under drought and saline conditions in accordance with the relative extremes of total soil water energy

Except for the uniform root distribution, all the root activity distributions specify the highest activities in the upper 25 cm, may give another explanation for the reduced values of PSI against the high SSI values (Tab.1 and fig. 3.2). The variably saturated zone might extend deeply until soil depth of 40 cm and in combination with the harsh extreme conditions in the topsoil, the area of zero root uptake and most active root uptake may be surrounded by the variably

saturated zone. The Surface crust, hysteresis phenomenon, and salt crystallization are the topsoil extremes and the high osmotic potential is the sub-soil extreme. All the latter extremes made the compensation insufficient to overcome the decrease in potential uptake.

3.3. Hysteresis and Relativity Phenomena in HASP

Under the conditions of time and/or depth are soil water potentials, available moistures, and accordingly soil water stress index, the changes in SSI with time and/or depth cause changes in water uptake, silicon passive uptake, and accordingly geo-alkaloids uptake (Figs. 3.1c, 3.1d, 3.4, 3.5, 3.6, and 3.7)

3.3.1. Hysteresis Phenomenon

In wetting drying cycles, time is a soil moisture, total soil water energy, soil stress index, and stressed water uptake response function. The soil moisture retention curve is different from wet to dry than from dry to wet at the same day in each irrigation cycle. This is as a response of signaling devices of plant hydraulic machinery systems toward the adopted soil moisture regime (Fig. 3.1f). As the time Progresses the soil moisture, soil stress index, and plant available water change due the evapotranspiration. The hysteresis phenomenon between wetting and drying conditions in each irrigation cycle takes place. (Homae *et al.*, 2002; Simunek and Radcliffe, 2010). In the structured soil, the intra-aggregate microstructure's nanoparticles (Peng *et al.*, 2022) are far away from the surficial tortuous preferential path of water. Hence, they need more time to respond to the added moisture. Plants may convert their canopies to the energy combination by which the evapotranspiration may be reduced touching the sustainable water use.

At the same soil depth, time as a moisture, and crop coefficient which was taken into account, soils revealed hysteresis phenomenon having different SSI values from irrigation cycle to another (Figs. 3.4, and 3.5) this may be attributed to:

1. **The different Spatial Connectivity of Pores During Wetting and Drying Processes** (Hillel, 2002 and Simunek et al., 2013).
2. **The Trapped Air** (Simunek and Radcliffe, 2010).
3. **The Contact Angle** (Nasr and Ati, 2023). The hysteresis in contact angle may cause hysteresis in PF-curve during (3.1e).
1) Add/remove a liquid volume to the drop without diminishing the interfacial area. 2) When a drop is applied to the surface then the surface is inclined, the drop is inclined uphill or downhill too. The difference in contact angle may cause hysteresis.
4. **Mesopores' Physisorption:** The quantity of adsorbed water differs when fluid is added during irrigation and when it is removed during evapotranspiration. In fact, the hysteresis in the mechanisms of water molecules physisorption during accumulation/evaporation processes occurring within only mesopores. Hysteresis is evidence of mesoporosity. (Gregg and Sing, 1982).
5. **Thixotropy Recovery:** A thixotropy is the property of water for becoming as thinner films in accordance with applied stress, strain, and weathered induced forces. After the dissipation of the latter forces the viscosity fully recovers it to its initial state in an appropriate period of time (Pham *et al.*, 2005).
6. **Hydration of Particles at Surfaces. – Hydration of Cations Inside Crystals.** They may give an explanation for hydraulic hysteresis (h_i) at ψ_m larger than 10 mpa (Lu and Khorshidi, 2015).
7. **The relationship between the uptake or hydrological release terms and water stress response functions** (Hegazy, 2020 and Peng et al., 2022).

3.3.2. Relativity of Albert Einstein

When plants' roots are doing responses to combined stresses of drought and salinity, they

change their locations in x, y, and z directions in order to uptake water and nutrients with minimum consumed energy. The different pulses of solute may be absorbed at different time from different depth's steps. With changing time and depth during the processes of water and nutrients' uptake, the soil moisture and its related characters and achieved parameters (HASP) exhibit a relativity of Albert Einstein in time and place during categorizing the energy states of soil water by plants' roots. Changing the time is a condition. Changing the location is another condition. Changing the time and place is another different condition. On the other words, Changing the time is a temporal variability. Changing the location is spatial variability. Changing the time and place is a tempospatial variability and it's a kind of relativity, the Albert relativity. Each of which has its appropriate value of absorbed water and solute according to the boundary conditions initial and final values of the upper and lower limits. The relativity of Albert Einstein's always matches the optimum approach (Dubbart *et al.*, 2023). Another different boundary conditions of tempospatial variability may be produced from the fact that each component in the agroecosystem is ordered to seek the optimality for the sake of serving mankind to let the life continue. Its another kind of relativity, the fate. Without it, the resurrection had been come and every thing is going to be at rest by the interrelated forces of global climatic changes.

Temporal and spatial variabilities of SSI and PSI can be obtained by executing the do loop iteration for equations (3.1, 3.2, and 3.6). The fact that soil helps plants to complete theirs under abiotic stress conditions to feed human and livestock in order to let the life continue is noticed (Figs 3.6 and 3.7). For one material soil profile, in the variably saturated zone, SSI changes with changing time and location. This may be attributed to Albert Einstein's relativity, the fourth type of soil response towards the applied drought stressor. When salinity stress

treatments were applied in combination with drought ones, all four soil responses might have been exceeded due to the additive concept of SSI. This might explain the obtained results that saline soil exhibited relativity and hysteresis in SSI higher than non-saline one (Figs. 3.4, 3.5, 3.6 and 3.7).

$$\int_Z^{Z+\Delta Z} SSI(t) dz = \int_Z^{Z+\Delta Z} SSI(t) dz = SSI_{(t)}^{(z+\Delta z)} - SSI_{(t)}^{(z)} = \begin{pmatrix} SSI_{(t)}^{(z+\Delta z)} \\ -SSI_{(t)}^{(z)} \end{pmatrix}$$

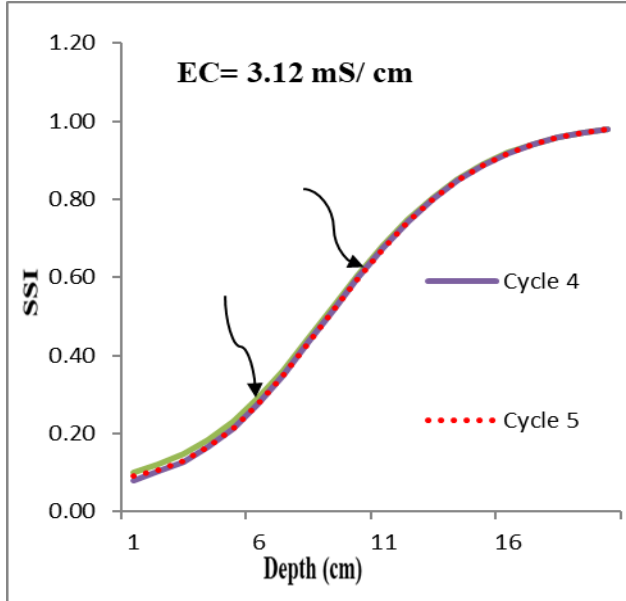


Figure (3.4): The variation of SSI with soil depth at the middle of irrigation cycle in non-saline soils.

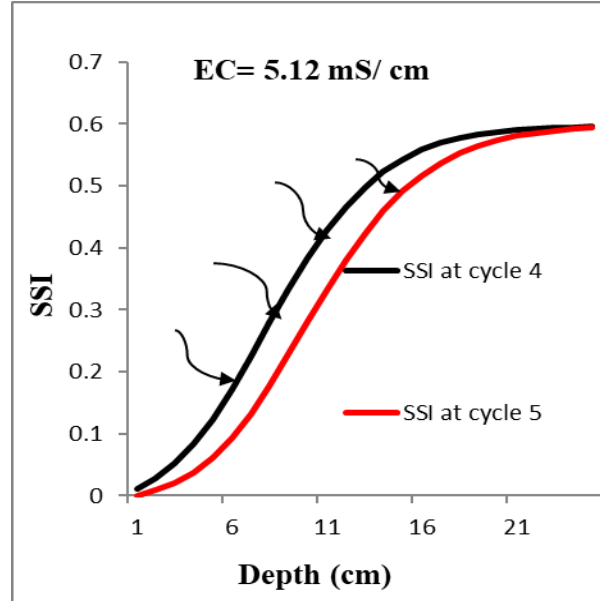


Figure (3.5): The variation of SSI with soil depth at the middle of irrigation cycle in saline soil.

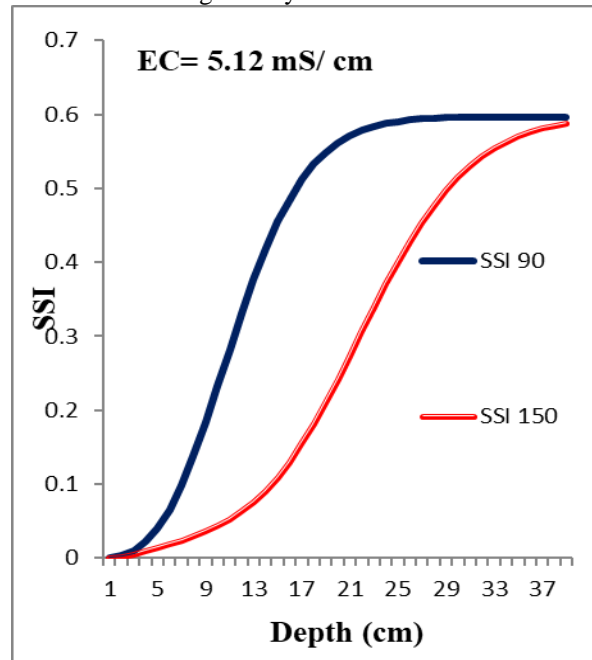
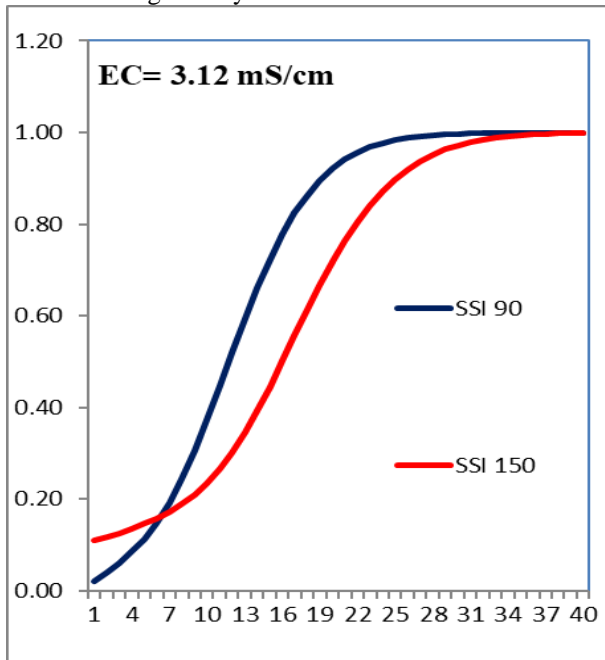


Figure (3.6): Albert Einstein’s relativity of SSI with depth and time in the variably saturated zone of non-saline soils.

Figure (3.7): Albert Einstein’s relativity of SSI with depth and time in the variably saturated zone of saline soils.

$$SSI_{z+\Delta z}^t - SSI_{z=1}^t = \left[\frac{(PSI)^{t_{z+\Delta z}} - \left[\frac{\sum_{z=1}^{z=n} (PSI)}{n} \right]}{KC \left[\frac{\sum_{z=1}^{z=n} (PSI)}{n} \right]} \right] * SSI_{z+\Delta z}^t$$

$$SSI_{zS}^t - SSI_{z=1}^t = \left[\frac{(PSI)^{t_{zS}} - \left[\frac{\sum_{z=1}^{z=n} (PSI)}{n} \right]}{KC \left[\frac{\sum_{z=1}^{z=n} (PSI)}{n} \right]} \right] * SSI_{zS}^t$$

$$SSI_{zN}^t - SSI_{z=1}^t = \left[\frac{(PSI)^{t_{zN}} - \left[\frac{\sum_{z=1}^{z=n} (PSI)}{n} \right]}{KC \left[\frac{\sum_{z=1}^{z=n} (PSI)}{n} \right]} \right] * SSI_{zN}^t$$

[3.1]

In the next incoming research chapter, equation (3.1) will be solved by Rung Kuta method the determine the relationship between PSI(z+Δz), SSI(z+Δz), and KC from PSI(z), SSI(z), Avg PSI, and KC.

Where:

SSI (i, j): Soil stress index in time and depth, respectively, PSI (i, j): Plant stress index in time and depth, respectively, n: Number of iterations. Kc: Crop coefficient, Time: i, Depth: j.

3.3.2.1.2. Constant Depth and Variable Time:

$$\int_t^{t+\Delta t} SSI(z) dt = \int_{z_t}^{z_t+\Delta z} SSI(z) dz = SSI_{(z)}^{(t+\Delta t)} - SSI_{(z)}^{(t)} = \begin{pmatrix} SSI_{(z)}^{(t+\Delta t)} \\ -SSI_{(z)}^{(t)} \end{pmatrix}$$

$$(SSI)_{t+\Delta t}^z - (SSI)_{t=1}^z = \left[\frac{(PSI)^{z_{t+\Delta t}} - \left[\frac{\sum_{t=1}^{t=n} ((n1*PSI1)+(n2*PSI2)+(n3*PSI3).....)}{n1+n2+n3+.....} \right]}{KC(t+\Delta t) \left[\frac{\sum_{t=1}^{t=n} ((n1*PSI1)+(n2*PSI2)+(n3*PSI3).....)}{n1+n2+n3+.....} \right]} \right] * (SSI)_{t+\Delta t}^z$$

[3.2]

In the next incoming research chapter, equation (3.2) will be solved by Rung Kuta method to determine the relationship between PSI(t+Δt), SSI(t+Δt), and KC(t+Δt) from SI(t), SSI(t), W. Avg. PSI, and KC(t).

Where:

SSI (t, z): Soil stress index in time and depth, respectively, PSI (t, z): Plant stress index in time and depth, respectively, n: Time (Days of each

growth stage). KC(t + Δt) : Crop coefficient due to the plants’ age starts from the first appear in lag phase until the disappear in dead phase.

The SF- RE including the sink/ source term (Eqs. 2.4) will be solved numerically in the further incoming research. The terms Avg PSI(Average PSI) and W. Avg (weighted average PSI) reflect the root adaptability against environmental abiotic stresses.

$$(SSI)_{t+\Delta t}^z - (SSI)_t^z = \begin{pmatrix} SSI^{((t+dt))} \\ (z) \\ SSI \\ (z) \end{pmatrix} = [h (K_1+K_2+K_3+K_4)]/6 \tag{3.3}$$

Where:

$K_1, K_2, K_3,$ and K_4 slops of four order Rung Kula (Fig. 3.8). As the left-hand sides in

equations (3.1, 3.2, and 3.3) are equal, the right-hand sides are equal too. Then

$$\frac{(PSI)^{t_{z+\Delta z}} - \left[\frac{\sum_{z=1}^{z=n} (PSI)}{n} \right]}{KC \left[\frac{\sum_{z=1}^{z=n} (PSI)}{n} \right]} * SSI_{z+\Delta z}^t = [h (K_1+K_2+K_3+K_4)]/6 \tag{3.4}$$

$$\frac{(PSI)^z_{t+\Delta t} - \left[\frac{\sum_{t=1}^{t=n} ((n1*PSI1)+(n2*PSI2)+(n3*PSI3).....)}{n1+n2+n3+.....} \right]}{KC(t+\Delta t) \left[\frac{\sum_{t=1}^{t=n} ((n1*PSI1)+(n2*PSI2)+(n3*PSI3).....)}{n1+n2+n3+.....} \right]} * (SSI)_{t+\Delta t}^z = [h (K_1+K_2+K_3+K_4)]/6 \tag{3.5}$$

Where:

1. $KC(t + \Delta t),$
2. $KC(t),$
3. $h (K_1+K_2+K_3+K_4)]/6 ,$
4. $\left[\frac{\sum_{z=1}^{z=n} (PSI)}{n} \right],$
5. $\left[\frac{\sum_{t=1}^{t=n} ((n1*PSI1)+(n2*PSI2)+(n3*PSI3).....)}{n1+n2+n3+.....} \right],$

Are known, the relationship between plant stress index and soil stress index is well extrapolated.

3.3.2.1.3. Variable Time and Depth:

$$\iint_{(z)(t)}^{(z+\Delta z),(t+\Delta t)} SSI dzdt = (SSI_{(t)}^{(z+dz)} - SSI_{(t)}^{(z)}) (SSI_{(z)}^{(t+dt)} - SSI_{(z)}^{(t)})$$

$$SSI_{z+\Delta z}^t - SSI_z^t = \left[\frac{(PSI)^{t_{z+\Delta z}} - \left[\frac{\sum_{z=1}^{z=n} (PSI)}{n} \right]}{KC \left[\frac{\sum_{z=1}^{z=n} (PSI)}{n} \right]} \right] * SSI_{z+\Delta z}^t$$

$$(SSI)_{t+\Delta t}^z - (SSI)_t^z = \left[\frac{(PSI)^z_{t+\Delta t} - \left[\frac{\sum_{t=1}^{t=n} ((n1*PSI1)+(n2*PSI2)+(n3*PSI3).....)}{n1+n2+n3+.....} \right]}{KC(t+\Delta t) \left[\frac{\sum_{t=1}^{t=n} ((n1*PSI1)+(n2*PSI2)+(n3*PSI3).....)}{n1+n2+n3+.....} \right]} \right] * (SSI)_{t+\Delta t}^z$$

Accordingly,

$$\iint_{(z)(t)}^{(z+\Delta z),(t+\Delta t)} SSI dzdt = \begin{pmatrix} SSI^{(z+dz)} \\ (t) \\ SSI \\ (z) \end{pmatrix} \begin{pmatrix} SSI^{((t+dt))} \\ (z) \\ SSI \\ (t) \end{pmatrix} = [h (K_1+K_2+K_3+K_4)]/6$$

$$= \left(\left[\frac{(PSI)^{t_{z+\Delta z}} - \left[\frac{\sum_{z=1}^{z=n} (PSI)}{n} \right]}{KC \left[\frac{\sum_{z=1}^{z=n} (PSI)}{n} \right]} \right] * SSI_{z+\Delta z}^t \right) . \left(\left[\frac{(PSI)^z_{t+\Delta t} - \left[\frac{\sum_{t=1}^{t=n} ((n1*PSI1)+(n2*PSI2)+(n3*PSI3).....)}{n1+n2+n3+.....} \right]}{KC(t+\Delta t) \left[\frac{\sum_{t=1}^{t=n} ((n1*PSI1)+(n2*PSI2)+(n3*PSI3).....)}{n1+n2+n3+.....} \right]} \right] * (SSI)_{t+\Delta t}^z \right) \tag{3.6}$$

a fourth order Runge-Kutta method

A fourth order Runge-Kutta method proceeds in four stages:

$$\begin{cases} k_1 = f(x_n, y_n) \\ k_2 = f(x_n + h/2, y_n + (h/2)k_1) \\ k_3 = f(x_n + h/2, y_n + (h/2)k_2) \\ k_4 = f(x_n + h, y_n + hk_3) \\ y_{n+1} = y_n + \frac{h}{6} (k_1 + 2k_2 + 2k_3 + k_4). \end{cases}$$

Figure (3.8): A four order Rung-kuta approximation method

But in fact, the extrapolations of SSI and PSI variabilities from non-hysteric and/ or non-relative data may differ than the extrapolations of SSI and PSI variabilities from hysteric and/ or -relative ones. The hysteresis and relativity in soil water potential may produce hysteresis and relativity in SSI, PSI, water and geo-akaloids' uptake , and finally water stress reduction function. The latter phenomena depend mainly on soil texture, structure, origin, and development. Similarly, the sink terms of the

stress form of Richard's equation (Eqs. 1, 2, and 3), $S = \beta \cdot SSI$, may be solved to extrapolate the temporal and spatial variabilities in water uptake reduction function. The latter may be achieved by replacing the term SSI in the equations (3.1, 3.2, 3.3, 3.4, 3.5, and 3.6) with the term $S_w = (\beta \cdot SSI)$ or $S_{si} = (\beta_{si} \cdot SSI)$ the results are temperal and spatial variabilitie in water uptake or silicon uptake, respectively. The temporal and spatial variabilities in geoalkaloids uptake may be also predicted (Hegazy, 2023)

$$\iint_{(z)(t)}^{(z+\Delta z),(t+\Delta t)} \beta \cdot SSI(z, t) dzdt = \left[\begin{pmatrix} (\beta SSI)_{(t+1)}^{(z+\Delta z)} \\ -(\beta SSI)_{(t)}^{(z+1)} \end{pmatrix} - \begin{pmatrix} (\beta SSI)_{(t+1)}^{(z)} \\ -(\beta SSI)_{(t)}^{(z)} \end{pmatrix} \right] \Delta t \Delta z = \left[\begin{pmatrix} (S)_{(t+1)}^{(z+\Delta z)} \\ -(S)_{(t)}^{(z+1)} \end{pmatrix} - \begin{pmatrix} (S)_{(t+1)}^{(z)} \\ -(S)_{(t)}^{(z)} \end{pmatrix} \right] \Delta t \Delta z$$

3.3.2.1.4. Intrinsic Variability:

$$S = \beta * SSI$$

$$\int_{(SSI)}^{(SSI+\Delta SSI)} S dSSI = \int_{(SSI)}^{(SSI+\Delta SSI)} \beta * SSI dSSI$$

$$\int_{(SSI)}^{(SSI+\Delta SSI)} S dSSI = 1/2 \int_{(SSI)}^{(SSI+\Delta SSI)} \beta d(SSI)^2$$

$$= 1/2 [\beta * (SSI)^2 - \int_{(SSI)}^{(SSI+\Delta SSI)} (SSI)^2 d\beta]_{(SSI)}^{(SSI+\Delta SSI)}$$

$$= 1/2 [\beta * (SSI)^2 + \alpha * Tp \int_{(SSI)}^{(SSI+\Delta SSI)} (SSI)^2 * (SSI)^{-2} dssi]_{(SSI)}^{(SSI+\Delta SSI)}$$

$$= 1/2 [\beta * (SSI)^2 + \alpha * Tp * SSI]_{(SSI)}^{(SSI+\Delta SSI)}$$

$$\therefore S \left(\frac{SSI^{(SSI+\Delta SSI)}}{SSI^{(SSI)}} \right) = 1/2 \left(\frac{\beta^{SSI+\Delta SSI} (SSI)^{2(SSI+\Delta SSI)} + \alpha 2Tp 2 * (SSI)^{SSI+\Delta SSI}}{-\beta SSI (SSI)^2 (SSI) - \alpha 1Tp 1 * (SSI)^{(SSI)}} \right)$$

$$\therefore S_w = \frac{\left(\frac{\beta^{SSI+\Delta SSI} (SSI)^{2(SSI+\Delta SSI)} + \alpha 2Tp 2 * (SSI)^{SSI+\Delta SSI}}{-\beta SSI (SSI)^2 (SSI) - \alpha 1Tp 1 * (SSI)^{(SSI)}} \right)}{2 \left(\frac{SSI^{(SSI+\Delta SSI)}}{SSI^{(SSI)}} \right)}$$

[3.7]

$$S_{Si} = \frac{\left(\begin{matrix} \beta_{Si} SSI + \Delta SSI (SSI)^2 (SSI + \Delta SSI) + \alpha_2 T_{p2} * (SSI)^{SSI + \Delta SSI} \\ - \beta_{Si} SSI (SSI)^2 (SSI) - \alpha_1 T_{p1} * (SSI)^{SSI} \end{matrix} \right)}{2 \left(\begin{matrix} SSI (SSI + \Delta SSI) \\ SSI (SSI) \end{matrix} \right)} \quad [3.8]$$

Where:

SSI: Soil stress index, β : Soil water hydraulic capacitance , β_{Si} : Silicon hydraulic capacitance
 ,, $\Delta SSI = SSI_2 - SSI_1 = SSI^{(SSI + \Delta SSI)} - SSI^{(SSI)}$, α_1 , α_2 , T_{p1} , and T_{p2} are plant stress

indices and potential transpiration constants for corresponding values of soil.

3.3.2.1.5. Stress Form of Richard’s Equation in Temporal and Spatial Variability

$$= \iint_{(t),(z)}^{(t+dt),(z+dz)} \left[\frac{b(t)}{b(z)} (dSSI + b(z).d/dz) dz . dt - \iint_{(t),(z)}^{(t+dt),(z+dz)} (\beta . SSI) dz . dt \right]$$

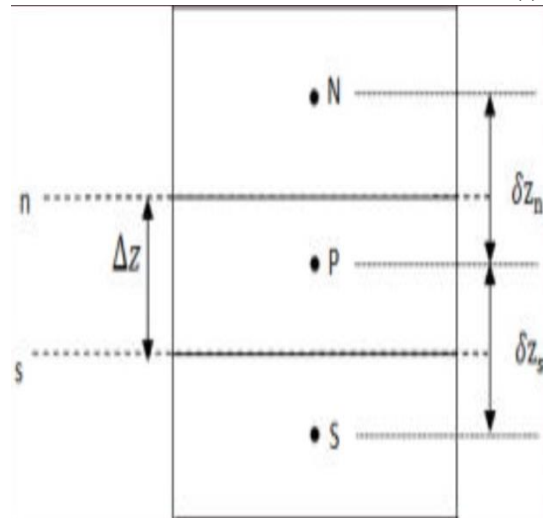


Figure (3.9): A portion of 1D Grid

$$\iint_{(t),(z)}^{(t+dt),(z+dz)} (C (SSI) \frac{dSSI}{dt}) . dz . dt$$

$$\int_z^{z+\Delta z} [(C(SSI).dSSI)^{t+dt} - (C(SSI).dSSI)^t] dz$$

throughout the control volume (Bazaraa *et al.*, 2015).

Where:

The finite volume concept suppose the whole specification of fluid and media is constant

$$\therefore \int_z^{z+\Delta z} [(C(SSI).dSSI)^{t+dt} - (C(SSI).dSSI)^t] dz$$

$$= \left(\begin{matrix} (C(SSI).dSSI)^{t+dt} \\ -(C(SSI).dSSI)^t \end{matrix} \right)_p . \Delta z$$

$$\int_t^{t+\Delta t} \int_{z,z}^{z+\Delta z} \left[\frac{b(t)}{b(z)} (dSSI + b(z)) \cdot d/dz \right] dz \cdot dt =$$

$$\left[\int_t^{t+\Delta t} \left[\frac{b(t)}{b(z)} (dSSI + b(z)) \right] \left(\frac{dz}{dz} \right) \cdot dt \right] =$$

$$= \int_t^{t+\Delta t} \left(\begin{matrix} \left(\frac{b(t)}{b(z)} (dSSI + b(z)) \right)_s \\ - \left(\frac{b(t)}{b(z)} (dSSI + b(z)) \right)_n \end{matrix} \right) dt$$

Note that:

time dependent and should be specified according to depth, north and south.

Despite of the homogeneity in the finite volume, the second term of the Richard's equation is

$$\therefore = \left(\begin{matrix} \left(\frac{b(t)}{b(z)} (dSSI+b(z)) \right)^{t+\Delta t} \\ - \left(\frac{b(t)}{b(z)} (dSSI+b(z)) \right)^t \end{matrix} \right)_s \Delta t = \left(\begin{matrix} \left((k(h)/dz (dSSI+b(z)))^{t+\Delta t} \right) \\ - \left((k(h)/dz (dSSI+b(z)))^t \right) \end{matrix} \right)_s \Delta t$$

$$= \left(\begin{matrix} \left(\frac{b(t)}{b(z)} (dSSI+b(z)) \right)^{t+\Delta t} \\ - \left(\frac{b(t)}{b(z)} (dSSI+b(z)) \right)^t \end{matrix} \right)_n \Delta t = \left(\begin{matrix} \left((k(h)/dz (dSSI+b(z)))^{t+\Delta t} \right) \\ - \left((k(h)/dz (dSSI+b(z)))^t \right) \end{matrix} \right)_n \Delta t$$

$$= \left(\begin{matrix} [kh^t \left(\frac{dSSI+b(z)}{dz} \right)]_s^{t+\Delta t} \\ - [kh^t \left(\frac{dSSI+b(z)}{dz} \right)]_n^{t+\Delta t} \end{matrix} \right) \Delta t$$

$$\therefore \left(\begin{matrix} (C(SSI) \cdot dSSI)^{t+\Delta t} \\ - (C(SSI) \cdot dSSI)^t \end{matrix} \right)_p \cdot \Delta Z = \left(\begin{matrix} [kh_s^t \left(\frac{dSSI+b(z)}{dz} \right)]_s^{t+\Delta t} \\ [kh_n^t \left(\frac{dSSI+b(z)}{dz} \right)]_n^{t+\Delta t} \end{matrix} \right) \Delta t$$

$$[kh_s^t \left(\frac{dSSI + b(z)}{dz} \right)]_s^{t+\Delta t} = kh_s^t \cdot \left[\left(\frac{dSSI + b(z)}{dz} \right)]_s^{t+\Delta t} - \left(\frac{dSSI + b(z)}{dz} \right)]_p^{t+\Delta t} \right]$$

$$[kh_n^t \left(\frac{dSSI + b(z)}{dz} \right)]_n^{t+\Delta t} = kh_n^t \cdot \left[\left(\frac{dSSI + b(z)}{dz} \right)]_p^{t+\Delta t} - \left(\frac{dSSI + b(z)}{dz} \right)]_n^{t+\Delta t} \right]$$

Where:

SSI^t and b(z)^t denote the value of SSI and b(z) at time t, respectively, Δt is the time step, SSI^(t+Δt) denotes the SSI at time t + Δt and the solution is assumed to be known at time level t

and unknown at time level t + Δt. Because the velocity of water flow in soil is very small, it is logical to consider K and accordingly, b(z) are constant during a time step.

$$\therefore \left(\begin{matrix} (C(SSI) \cdot dSSI)^{t+\Delta t} \\ - (C(SSI) \cdot dSSI)^t \end{matrix} \right)_p \cdot \Delta Z = \left(\begin{matrix} kh_s^t \cdot \left[\left(\frac{dSSI+b(z)}{dz} \right)]_s^{t+\Delta t} - \left(\frac{dSSI+b(z)}{dz} \right)]_p^{t+\Delta t} \right) \Delta t$$

$$- kh_n^t \cdot \left[\left(\frac{dSSI+b(z)}{dz} \right)]_p^{t+\Delta t} - \left(\frac{dSSI+b(z)}{dz} \right)]_n^{t+\Delta t} \right) \Delta t$$

$$\therefore C(SSI)_p^t \left(\begin{matrix} (dSSI)_p^{t+\Delta t} \\ - (dSSI)_p^t \end{matrix} \right) \cdot \Delta Z = \left(\begin{matrix} kh_s^t \cdot \left[\left(\frac{dSSI+b(z)}{dz} \right)]_s^{t+\Delta t} - \left(\frac{dSSI+b(z)}{dz} \right)]_p^{t+\Delta t} \right) \Delta t$$

$$- kh_n^t \cdot \left[\left(\frac{dSSI+b(z)}{dz} \right)]_p^{t+\Delta t} - \left(\frac{dSSI+b(z)}{dz} \right)]_n^{t+\Delta t} \right) \Delta t$$

$$\begin{aligned} \left(\begin{matrix} (dSSI)_p^{t+dt} \\ - (dSSI)_p^t \end{matrix} \right) &= \frac{1}{C(SSI)_p^t} \left(\begin{matrix} kh_s^t \cdot \left[\left(\frac{dSSI+b(z)}{dz} \right)_s^{t+\Delta t} - \left(\frac{dSSI+b(z)}{dz} \right)_p^{t+\Delta t} \right] \\ - kh_n^t \cdot \left[\left(\frac{dSSI+b(z)}{dz} \right)_p^{t+\Delta t} - \left(\frac{dSSI+b(z)}{dz} \right)_n^{t+\Delta t} \right] \end{matrix} \right) \frac{\Delta t}{\Delta z} \\ (dSSI)_p^{t+dt} &= \frac{1}{C(SSI)_p^t} \left(\begin{matrix} kh_s^t \cdot \left[\left(\frac{dSSI+b(z)}{dz} \right)_s^{t+\Delta t} - \left(\frac{dSSI+b(z)}{dz} \right)_p^{t+\Delta t} \right] \\ - kh_n^t \cdot \left[\left(\frac{dSSI+b(z)}{dz} \right)_p^{t+\Delta t} - \left(\frac{dSSI+b(z)}{dz} \right)_n^{t+\Delta t} \right] \end{matrix} \right) \frac{\Delta t}{\Delta z} + (dSSI)_p^t \end{aligned}$$

Similary,

$$\begin{aligned} \text{The sink term} &= \iint_{(z)(t)}^{(z+\Delta z),(t+\Delta t)} \beta \cdot SSI(z, t) dz dt = \left[\left(\beta SSI \right)_{(t+1)}^{(z+\Delta z)} - \left(\beta SSI \right)_{(t+1)}^{(z)} \right] \Delta t \Delta z \\ &= \left[\left(\begin{matrix} (S) \\ - (S) \end{matrix} \right)_{(t+1)}^{(z+\Delta z)} - \left(\begin{matrix} (S) \\ - (S) \end{matrix} \right)_{(t+1)}^{(z)} \right] \Delta t \Delta z = [(S)_p^{t+dt} - (S)_p^t] \Delta t \Delta z = [(\beta \cdot SSI)_p^{t+dt} - (\beta \cdot SSI)_p^t] \Delta t \Delta z \\ &= \iint_{(z)(t)}^{(z+\Delta z),(t+\Delta t)} \beta \cdot SSI(z, t) dz dt = [(\beta \cdot SSI)_p^{t+dt} - (\beta \cdot SSI)_p^t] \Delta t \Delta z \end{aligned}$$

3.3.2.1.6. Solution Stress Form of Richard’s Equation in Temporal , Spatial , and Intrinsic Variability:

Similarly,

$$\begin{aligned} &\iiint_{(t),(z),(SSI)}^{(t+dt),(z+dz),(SSI+dSSI)} C(SSI) \frac{dSSI}{dt} dSSI \cdot dz \cdot dt \\ &= \iiint_{(t),(z),(SSI)}^{(t+dt),(z+dz),(SSI+dSSI)} k(h) \frac{dSSI + b(z)}{dz} dSSI \cdot dz \cdot dt \\ &- \iiint_{(t),(z),(SSI)}^{(t+dt),(z+dz),(SSI+dSSI)} (\beta \cdot SSI) dSSI \cdot dz \cdot dt \end{aligned}$$

4. Conclusion

Anthropogenic gas emissions will change the earth's atmosphere taking it off from its blue and green fascinating colors, dressing it the garment of the yellow harsh extreme desertification, and mammalian uninhibited regions due to the global temperature rise. Drought and salinization are results of global climatic changes. They could negatively affect the agricultural production. Managerial practices under such conditions involve the foliar application of silicon to enhance crop yield and plantation properties. The agro-ecosystem continuum, plant, soil, and atmosphere interact altogether in order to mitigate the impact of abiotic stressors. The geo-temporal variabilities impose special managerial tools to

be detected in order to adopt the appropriate technology dealing with any certain interrelated problem to climatic changes. SF-RE created by the author contains four newborn abiotic stress parameters, SSI, β, bz, and bt. It's the moisture redistribution (bz) which makes the curvature of SSI in the root domain becomes gradual and hence saves plants life as long as possible now and then each wetting drying cycles. It's the gaining factor (bt) which determines appropriated moisture regimes should be applied in the deficit irrigation scenarios without causing a reliable reduction in crop yield and plantation properties. It's the soil stress index which determines types and amounts of water and nutrients' uptake according to the logical model of the relative extreme total soil water energy. Finally, it's the soil water hydraulic

capacitance which determines types and amounts of water and nutrients' uptake in accordance with stress, strain, and weather induced forces. As plant stress index is the dependent variable of soil stress index, values of plant stress index were predicted using the corresponding values of soil stress index. Discretization equations between SSI and PSI were created in one and two dimensions. The SF-RE in tempospatial variabilities was solved using the finite volume approximation. Relativity and hysteresis were found and discussed using the optimal approaches of modeling. Roots' water and nutrients' uptake, SSI, PSI, bz, and bt exhibited intrinsic variabilities. These variabilities may be attributed to the inherited geosignal of total **soil water energy**. Under the stressors of global climatic changes, **Kingdoms planta and animalia** interact either alone or in combination with the other agroecosystems' components, soil, water, and atmosphere seeking the optimality which let the life continue till the order come. When He order, all the positive responses will follow the direction of the negativity. The flow of energy and matter will be coming with obedience for the resurrection, the rest. Therefore, there won't be any optimality. It's the end of life on planet earth. **Sunshine, not only is being the source of all energies and lives on planet earth but also the optimistic behavior of ours.**

Funding

No funding

Institutional Review Board Statement

All Institutional Review Board Statements are confirmed and approved.

Data Availability Statement

Data presented in this study are available on fair request from the respective author.

Ethics Approval and Consent to Participate

Not applicable

Consent for Publication

Not applicable.

Conflicts of Interest

The author disclosed no conflict of interest.

4. References

- Abaghandura, G., D. Park, D. White, and W. Bridges. (2017). Modelling soil degradation in Libya. *J. Natu. Sci. Res.*, (7) 24: 30-40.
- Albasha, R., I. C. Mailhol, and B. Cheviron. (2015). Compensatory uptake functions in empirical macroscopic root water uptake models- experimental and numerical analysis.
- Bazaraa, A. (2015). Lectures in unsaturated zone hydrology, Part one, Faculty of Engineering, Cairo University.
- Berard, M. and G. Girard. (2024). Modeling plant water deficit by a non-local root water uptake term in the unsaturated flow equation. *Communications in Nonlinear Science and Numerical Simulation*, 128 (2024) 107583. Availavle at: [Modeling plant water deficit by a non-local root water uptake term in the unsaturated flow equation \(sciencedirectassets.com\)](https://www.sciencedirect.com/science/article/abs/pii/S0960077924001583)
- Biard, T., J. W. Krause, M. R. Stukel, and M. D. Ohman. (2018). The Significance of giant Phaeodarians (Rhizaria) to Biogenic Silica Export in the California Current Ecosystem. *Global Biogeochemical Cycles*. Available at: <https://doi.org/10.1029/2018GB005877>
- El-Khader, M. (2015). Lectures in unsaturated zone hydrology, Part three. Faculty of Engineering, Cairo University.
- El-Sokkary, I. H. (2018). Silicon as a beneficial element and as an essential plant nutrient: An outlook. *Alex. Sci. Exch. J.* 39: 534-550
- Epstein, E. (2009). Silicon: its manifold roles in plants. *Ann. Appl. Biol.*, 155: 155–160.
- FAO. (2002). *Crops and Drops: Making the Best Use of Water for Agriculture*. Food and Agriculture Organization of the United Nations, Rome, Italy. <http://www.fao.org>.

- Farnsworth, A., Y. T. Eunice Lo, P. J. Valdes, J. R. Buzan, P. J. Mills, A. S. Merdith, C. R. Scotese, and H. R. Wakeford. (2023). Climate extremes likely to drive land mammal extinction during next supercontinent assembly. *Nature Geoscience*, Vol (16): 901–908. Available at : <https://doi.org/10.1038/s41561-023-01259-3>
- Gregg, S. and K. Sing. (1982). Adsorption, Surface Area, and Porosity (Second ed.). London: Academic Press
- Hegazy, El-Sh. M. (2002). Effect of organic conditioners on some soil physical properties and loss of nutrient elements by leaching. M.Sc. Thesis, Faculty of Agriculture, Saba Basha, Alexandria University.
- Hegazy, El-Sh. M. (2020). Modeling the response of root uptake to silicon foliar application under drought and saline conditions in Egypt and Libya. Ph.D. Thesis, Faculty of African Postgraduate Studies, Cairo University, Giza, Egypt.
- Hegazy, El-Sh. M. (2022a). Modelling the response of root uptake to silicon foliar application under drought and saline conditions in Egypt and Libya. Lap-Lambert Academic Publishing, Moldova. Available at: <https://www.morebooks.de/shop-ui/shop/product/9786204746456>
- Hegazy, El-Sh. M. (2022b). New Valuable Tools for Assessing Some Environmental Impacts of Global Climatic Changes on the Agro-Ecosystem's Continuum. Lap-Lambert Academic Publishing, Moldova. Available at: <https://www.morebooks.de/shop-ui/shop/product/9786205501139>
- Hegazy, El-Sh. M. (2023). Modelling the plant silicon hydraulic capacitance and passive uptake under drought and saline conditions. *Global Journal of Science Frontier Research: D Agriculture and Veterinary*, Vo (23) Iss. (3) Ver. (1). Available at : [GlobalJournalofScienceFrontierResearch\(globaljournals.org\)](http://GlobalJournalofScienceFrontierResearch(globaljournals.org))
- Hegazy, El-Sh. M. (2024). Modeling Plant's Water And Nutrients Uptake Using Stress Form Of Richard's Equation. Lap-Lambert Academic Publishing, Moldova. Available at: www.morebook.com
- Hillel, D. (2002). Environmental of Soil Physics. Academic Press Inc., New York, 550 p.
- Homaei, M., R. A Feddes, and C. Dirksen. (2002). Simulation of root water uptake. II Non- uniform transient water stress using different reduction functions. *Agric. W. Mang.*, 57:111- 126.
- Intergovernmental Panel on Climate Change. (2023). Synthesis Report. Contribution of Working Groups I, II and III to the Sixth Assessment Report of the Intergovernmental Panel on Climate Change [Core Writing Team, H. Lee and J. Romero (eds.)]. IPCC, Geneva, Switzerland, pp. 35-115, doi: 10.59327/IPCC/AR6-9789291691647.
- Jarvis, N.J. (2010). Comment on “Macroscopic root water uptake distribution using matrix flux potential approach”. *Vadose Zone J.*, 9: 499–502.
- Liang Y., W. Sun, Y-G. Zhu, and P. Christie. (2007). Mechanisms of silicon alleviation of abiotic stresses in higher plants: A review. *Environ. Pollut.*, 147: 422-428.
- Lu, N. and M. Khorshidi. (2015). Mechanisms for soil-water retention and hysteresis at high suction range. *Journal of Geotechnical and Geoenvironmental Engineering*. 141(8): 04015032.
- Nasr, M. M. and A. S. Ati. (2023). Hysteresis in Soil, Its Causes and Influences IOP Conf. Ser.: Earth Environ. Sci. 1262 082052
- Peter, A. (2016). Modified conceptual model for compensated root water uptake – a simulation study. *J.of Hydrology*, 534: 1-10.
- Peters, A., W. Durner, and S. C. Iden, (2017). Modified Feddes type stress reduction function for modelling root water uptake:

- Accounting for limited aeration and low water potential. *Agric. Water Manag.*, 185: 126- 136.
- Peng, J., X. Wu, S. Ni, J. Wang, Y. Song, and Ch. Cai, (2022). Investigating intra-aggregate microstructure characteristics and influencing factors of six soil types along a climatic gradient. *Catena* 210 (2022) 105867.
- Pour, M. A., M. M. Shoshtari, and M. Adib. (2011). Numerical solution of Richard's equation by using of finite volume method. *World Applied Sciences Journal* 14 (12) : 1838-1842.
- Pham, H., D. Fredlund, and S. Barbour. (2005). A study of hysteresis models for soil- water characteristic curves. *Canadian Geotechnical Journal*. 42(6): 1548-1568.
- Simunek, j. and J.W Hopmans,. (2009). Modelling compensated root water and nutrient uptake. *Ecological Modelling*, 22: 505–521.
- Simunek, J. and E. Radcliffe . (2010). *Soil Physics with Hydrus, Modelling and Applications*. CRC Press, Boca Raton, Florida.
- Simunek, J., M. Sejna, H. Saito, M. Sakai, and M. Th. Van Genuchten, (2013). *The HYDRUS-1D Software Package for Simulating the One-Dimensional Movement of Water, Heat, and Multiple Solutes in Variably-Saturated Media*. Version 4.17. Department of Environmental Sciences University of California Riverside, p. 240.
- Sposito, G. (2008). *The Chemistry of Soils*. 2nd edition. Oxford University Press, New York, p. 180, 296,297.
- Szymkiewicz, A. (2013). Modelling water flow in unsaturated porous media. Chapter 3:Numerical solution of flow equations. PP. 49. Available at: <http://www.springer.com/series/882>
- Tierney, J., C. J. Poulsen, I. P. Montañez, T. Bhattacharya, R. Feng, H. L. Ford, B. Hönisch, G. N. Inglis, S. V. Petersen, N. Sagoo, C. R. Tabor, K. Thirumalai, J. Zhu, N. J. Burls, G. L. Foster, Y. Goddérés, B. T. Huber, L. C. Ivany, S. K. Turner, D. J. Lunt, J. C. McElwain, B. J. W. Mills, B. L. Otto-Bliesner, A. Ridgwell, Y. G. Zhang. (2020). *Science*. Vol. (370), Iss. (6517). Available at: <https://doi.org/10.1126/science.aay3701>
- Thanh, H. Th. and G. L. Song. (2023). Calculating groundwater recharge using saturated-unsaturated flow modeling. *IOP Conf. Ser., Earth Environ. Sci.* 1226 (2023) 012027
- Van Genuchten, M.Th. (1987). A numerical model for water and solute movement in and below the root zone, Unpublished Research Report, U.S. Salinity Laboratory, USDA, ARS, Riverside, CA.
- Wang, X., H. Cai, Z. Zheng, L. Yu, Z. Wang, and L. Li. (2020). Modelling root water uptake under deficit irrigation and rewetting in Northwest China. *Agronomy Journal*, 112:158–174.
- Wu, X., J. Shi, O. Zuo, M. Zhang, X. Xue, L. Wang, T. Zhang, and A. BenGal.(2020). Parameterization of the water stress reduction function based on soil– plant water relations. *Irrigation Science*. <https://doi.org/10.1007/s00271-020-00689-w>
- Zarebanadkouki, M., M. Ahmed, C. Hedwig, P. Benard, S. J. Kostka, A. Kastner, and A. Carminati. (2018). Rhizosphere hydrophobicity limits root water uptake after drying and subsequent rewetting. *Plant Soil*, 428: 265–277. <https://doi.org/10.1007/s11104-018-3677-7>